permutation may have played a role in the evolution of these RNAs. Some RNA folding motifs may have evolved with very different termini prior to a rare event where a circular RNA intermediate is formed and cleaved at a different location to result in circularly permuted RNA. Subsequent reverse transcription could convert the circularly permuted motif back into DNA. Such events may explain the appearance of circularly permuted tRNA-like motifs in other RNAs or may suggest that tRNA itself originally appeared as a circularly permuted isomer.

REFERENCES AND NOTES

1. K. Luger, U. Hommel, M. Herold, J. Hofsteense, K. Kirschner, *Science* **243**, 206 (1989).
2. G. J. Quigley and A. Rich, *ibid.* **194**, 796 (1976).
3. S.-H. Kim, in *Transfer RNA*, S. Altman, Ed. (MIT Press, Cambridge, MA, 1978), pp. 248–293.
4. C. Werner *et al.*, *Biochim. Biophys. Acta* **432**, 161 (1976).
5. W. J. Krzyzosiak *et al.*, *Biochemistry* **27**, 5771 (1988).
6. R. S. Brown *et al.*, *ibid.* **24**, 4785 (1985).
7. L. S. Behlen *et al.*, *ibid.* **29**, 2515 (1990); L. S. Behlen and O. C. Uhlenbeck, unpublished results.
8. A. G. Bruce and O. C. Uhlenbeck, *Nucleic Acids Res.* **5**, 3665 (1978).
9. E. Westhof *et al.*, *J. Mol. Biol.* **184**, 119 (1985).
10. V. I. Ivanov *et al.*, *Biopolymers* **12**, 89 (1973); W. Saenger, *Principles of Nucleic Acid Structure* (Springer-Verlag, New York, 1984), pp. 368–384.
11. D. Gautheret *et al.*, *Cabios* **6**, 325 (1990).
12. T. Pan, A. DiRenzo, O. C. Uhlenbeck, unpublished results.
13. M. Springer *et al.*, *EMBO J.* **8**, 2417 (1989); F. Dardel *et al.*, *Mol. Gen. Genet.* **223**, 121 (1990).
14. T. W. Dreher and T. C. Hall, *J. Mol. Biol.* **201**, 31 (1988); T. W. Dreher *et al.*, *ibid.* **206**, 425 (1989).
15. J. R. Sampson *et al.*, *Cold Spring Harbor Symp. Quant. Biol.* **52**, 267 (1987).
16. M. W. Gray and M. N. Schnare, in *The Ribosome: Structure, Function and Evolution*, W. Hill *et al.*, Eds. (American Society for Microbiology, Washington, DC, 1990), pp. 589–597.
17. O. C. Uhlenbeck, *Nature* **328**, 596 (1987).
18. A. J. Zaug and T. R. Cech, *Science* **231**, 470 (1986).
19. A DNA plasmid encoding a G1A mutant of YF0 was transcribed by T7 RNA polymerase and purified as previously described (*20, 21*), except that a five-fold excess of adenosine 5′-monophosphate over adenosine triphosphate (ATP) was included in the transcription reaction to generate RNA with a 5′-monophosphate. In order to form an intramolecular circle, 10 μM linear tRNA was incubated in 50 mM tris, pH 7.6, 10 mM $MgCl_2$, 10 mM β-mercaptoethanol, 0.2 mM ATP, bovine serum albumin, (0.1 mg/ml) 15% dimethyl sulfoxide, and T4 RNA ligase (1 U/μl) for 2 hours at 37°C. In order to introduce a unique ^{32}P label at the Pb^{2+} cleavage site, 2 μM circular tRNA was cleaved in 15 mM MOPS, pH 7.0, 15 mM $MgCl_2$, and 0.4 mM lead acetate at 23°C for 6 min followed by ethanol precipitation to remove Pb^{2+}. The precipitated tRNA was then redissolved to 3.5 μM in 30 mM tris, pH 8.0, 15 mM $MgCl_2$, and T4 polynucleotide kinase (1.5 U/μl) and incubated for 45 min at 37°C. Upon addition of 30 mM tris, pH 7.5, 8 mM dithiothreitol, and [γ-^{32}P]ATP, the reaction mixture was further incubated at 37°C for another 30 min. The resulting tRNA with a ^{32}P label at its 5′ end and free 3′-OH, was then religated under conditions described above. Alkaline hydrolysis was carried out with 7 μM circular tRNA in 1 mM glycine, 0.4 mM $MgSO_4$, pH 9.5, by boiling for 45 s. The tRNA was renatured in 30 mM MOPS, pH 7.0, by heating for 2 min at 85°C. Lead cleavage was finally carried out under conditions as described in legend to Fig. 2 for 6 min at 23°C. The cleavage reaction was stopped by addition of an equal volume of 8 M urea and 50 mM EDTA, and the reaction mixture was then directly loaded onto a 10 or 20% polyacrylamide gel that contained 7 M urea. To ensure that no new Pb^{2+} cleavage site is generated upon circular permutation, it was necessary to show that all of the fragments shorter than full-length linear tRNA contained a 3′-terminal ^{32}P phosphate. This was done by incubating an aliquot of the lead-cleaved reaction mixture in 0.1 M HCl for 1 hour at 25°C to hydrolyze the 2′,3′-cyclic terminal phosphate, followed by neutralization with NaOH and treatment with 1 U of calf intestine alkaline phosphatase in 50 mM tris, pH 8.0, at 37°C for 1 hour. When the reaction mixture was analyzed by denaturing polyacrylamide gel electrophoresis, no radioactive bands other than the circular and full-length linear tRNAs were detected, showing that the 3′ ^{32}P was removed from all of the fragments.
20. J. F. Milligan and O. C. Uhlenbeck, *Methods Enzymol.* **180**, 51 (1989).
21. J. R. Sampson and O. C. Uhlenbeck, *Proc. Natl. Acad. Sci. U.S.A.* **85**, 1033 (1988).
22. Descriptor of the GenBank search: Both the anti-codon and acceptor stems were reduced to a minimum of 3 base pairs, and the acceptor and anticodon loops were permitted to vary between 3 and 28 bases; in addition, the α region in the D loop (nucleotides 16 and 17) was variable from 1 to 20 bases. Five of the nine tertiary base-base interactions in tRNA, U8-A14, R15-Y48, G18-U55, S19-S56 (G/C19-C/G56), and U54-A58, were retained in our search. G-U base pairs in helices and up to one mismatch in the T and two mismatches in the D stems were allowed.

23. Supported by NIH grant GM37552. T.P. is supported by a Damon Runyon–Walter Winchell Cancer Research Fund Fellowship, DRG-1103. We also thank the W. M. Keck Foundation for their generous support of RNA science on the Boulder campus. We thank D. Gautheret and R. Cedergren for making the program RNAMOT available for our GenBank search.

31 July 1991; accepted 4 October 1991

Viviparous Leaves Produced by Somatic Activation of an Inactive Cytokinin-Synthesizing Gene

JUAN JOSÈ ESTRUCH, ELS PRINSEN, HARRY VAN ONCKELEN, JEFF SCHELL, ANGELO SPENA*

Tobacco plants that are somatic mosaics for expression of a cytokinin-synthesizing gene have viviparous leaves. Such a formation of shoots in an abnormal position represents a significant deviation from the usual organization of the plant body where a central axis produces shoots only in the axils of lateral leaf appendages and according to a precise phyllotactic pattern. This report links vivipary to the expression of a gene whose product is involved in the synthesis of the phytohormone cytokinin.

UNDER NATURAL PLANT GROWTH conditions, leaves that form adventitious buds on their surfaces or edges are said to be viviparous (*1, 2*). Depending on the plant species, this manifestation of totipotency of differentiated leaf cells is a phenomenon occurring either as part of a normal developmental process (*3, 4*) or as a teratological event (*1*). Knowledge of the underlying cellular mechanisms is scant. We report here that vivipary is acquired by tobacco leaves that are somatic genetic mosaics for the expression of a cytokinin-synthesizing gene.

In culture with added growth regulators, leaf explants of several species express new developmental patterns (*5*). In particular, cytokinins are routinely used to regenerate plants from explants (*5*). Expression of cytokinin in vivo was altered here with the use of the crown gall *ipt* gene. Crown galls are neoplastic plant tissues resulting from the transfer and expression of oncogenes carried on a transferable DNA segment (T-DNA) of the Ti plasmid of the bacterial pathogen *Agrobacterium tumefaciens*. One of these oncogenes, *ipt*, codes for an isopentenyltransferase, which is involved in cytokinin synthesis (*6*). Expression of the *ipt* gene under the control of the 35*S* RNA promoter from cauliflower mosaic virus (CaMV) increases the cytokinin content up to 137 times in transgenic shoots of *Nicotiana tabacum, N. rustica*, and *N. plumbaginifolia* (*7*). These shoots exhibit loss of apical dominance and are unable to root (*7, 8*). The *ipt* gene under control of inducible (*9–11*) or tissue-specific promoters (*12*) circumvents the inhibitory effect of high endogenous levels of cytokinin on root formation. However, most inducible promoters have a low basal level of constitutive expression, and tissue-specific promoters have localized expression occurring only after differentiation, limiting the study of the influence of cytokinins on plant development.

We have inserted the maize transposon *Ac* (*13–16*), into the untranslated leader sequence of the 35*S-ipt* gene to inactivate the *ipt* gene (Fig. 1). Somatic transposon excision subsequently reactivates expression of the 35*S-ipt* gene. Whereas early excision events are expected to generate teratoma-like tissues unable to form roots, excision events taking place late in plant development

J. J. Estruch, J. Schell, A. Spena, MPI für Züchtungsforschung, Carl-von-Linne weg, 10, 5000 Köln 30, Germany. E. Prinsen and H. Van Onckelen, UIA, Universiteitsplein, B-2610 Antwerpen (Wilrijk), Belgium.

*To whom correspondence should be addressed.

should be compatible with plant regeneration and result in somatic genetic mosaics composed of clonal populations of cells expressing the *ipt* gene intermixed with cells that do not express it. With the use of somatic genetic mosaics, the effect of cytokinin content, whether synthesized locally or transported from other tissues, on the development of a clonal population of cells can be studied in plants. We have shown that an increased amount of cytokinin triggers shoot formation on leaves in planta.

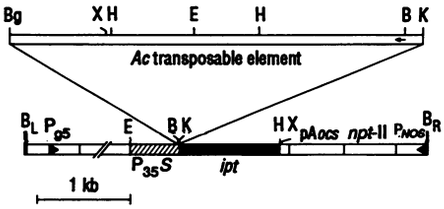

Fig. 1. The transposon-split 35*S-ipt* chimeric gene. The *Ac* transposon (*15, 16*) was inserted between the 35*S* RNA promoter from CaMV and the *ipt* coding region. The entire construction is located between the Eco RI and the Hind III sites of the binary vector pPCV002 (*25*). The small arrow indicates the direction of *Ac* transcription. Abbreviations: $P_{35}S$, CaMV 35*S* promoter; B_L and B_R, left and right border sequences of vector T-DNAs; P_{g5}, truncated promoter of T_L-DNA gene 5; P_{NOS}, promoter of nopaline synthase gene; pA*ocs*, polyadenylation sequence of octopine synthase gene; *npt*-II, neomycin phosphotransferase gene of transposon Tn*5*; B, Bam HI; Bg, Bgl II; E, Eco RI; H, Hind III; K, Kpn I; and X, Xba I.

Table 1. Cytokinin levels (±SE) in 35*S-Ac-ipt* transgenic tobacco plants. Plant material was homogenized in 75% methanol and 100 becquerel of H^3-zeatin-riboside dialcohol (ZRD) were added for recovery purposes. After centrifugation, the extract was passed through an RP-C18 column, evaporated in vacuo and dissolved in 35% ethanol. Anti-ZR radioimmunoassays (RIA) were performed as described in (*22*) with slight modifications. Anti-ZR-chicken egg yolk antibodies used were purified by thiophilic interaction chromatography (*23*). Trans-H^3-ZRD (40 Ci/mmol) was the radioactive tracer in the ZR-RIA. Samples were tested at seven dilutions. Standard curves are plotted after a logit transformation (*24*). ZR equivalents were measured in picomoles per gram formula weight.

Clone	Tissue	ZR equivalents
SR1	Nontransformed leaf	36 ±15 (n = 5)
Ac-ipt 12	Altered leaf tissue	131 ± 15 (n = 3)
Ac-ipt 12	Normal leaf tissue	29 ± 4 (n = 4)
Ac-ipt 5	Altered leaf tissue	127 ± 16 (n = 6)
Ac-ipt 3	Normal leaf tissue	17 ± 7 (n = 4)
Ac-ipt 5	Teratoma-like bud	3300 ± 400 (n = 4)

Of 80 kanamycin-resistant transgenic shoots obtained by transformation of tobacco leaf disks with the 35*S-Ac-ipt* construct (Fig. 1), 39 degenerated into leafy teratomas. Twenty were able to form roots in vitro; however, only eight survived after transfer to soil. All eight surviving plants displayed developmental and morphological alterations such as loss of apical dominance and leaf blade bulges intermixed with normal tissue. Four transgenic tobacco clones managed to set seeds. DNA extracted from phenotypically altered leaf tissues (Fig. 2, A and B) showed that these tissues harbored a reconstituted 35*S-ipt* gene resulting from excision of the *Ac* element from the original construct. DNA from normal tissue contained only the 35*S-Ac-ipt* construct (Fig. 2, A and B). RNA blot analysis demonstrates the presence of *ipt* homologous transcripts in polyadenylated [poly(A)$^+$] RNA extracted from altered-leaf tissues, but not from normal parts of tobacco leaves (Fig. 2C). The *ipt* protein must be active because the amounts of cytokinins detected in such altered-leaf areas are higher than those in nonaltered leaf areas and those in nontransformed SR1 tobacco leaves (Table 1). These findings indicate that the observed phenotype in leaf mesophyll tissue resulted from a somatic genetic mosaicism for the expression of the *ipt* gene.

The formation of adventitious buds in 35*S-Ac-ipt* transgenic tobacco leaves may be caused either by *ipt* gene expression in the cell or cells generating the new meristemoids or by cytokinin produced elsewhere and transported along the vascular system. Northern blot analysis shows that *ipt* gene transcripts could be detected in six of eight adventitious buds analyzed (Fig. 2D). Nevertheless, hormonal analysis detected high amounts of cytokinins in an adventitious bud (Table 1). Furthermore, exogenous application of radioactive cytokinins to the vascular tissue of leaf petioles resulted in an accumulation of radioactivity at the tip of the leaves. Hence, adventitious bud formation does not necessarily require *ipt* gene expression in the actual cells that generate the bud, but it could be triggered by cytokinin synthesized in other parts of the plant and transported acropetally. This conclusion supports the notion that the presence and not the production of a growth regulator in

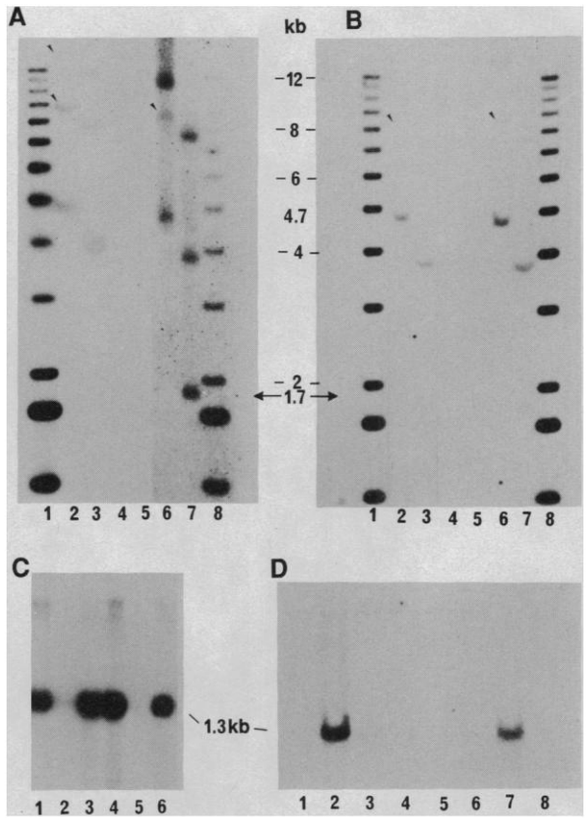

Fig. 2. DNA and RNA gel blot analysis (*26*) of 35*S-Ac-ipt*–containing transgenic plants. (**A**) Southern DNA hybridization of tissue from a single leaf from transgenic plant clone 35*S-Ac-ipt* 19. Lanes 1 and 8, DNA radiolabeled markers; lanes 2, 4, and 6, Xba I digests; lanes 3, 5, and 7, Xba I-Eco RI digests of genomic DNA. Samples from morphologically normal transgenic leaf tissue (lanes 2 and 3), control SR1–wild-type leaf tissue (lanes 4 and 5), and altered transgenic leaf tissue (lanes 6 and 7). The probe was 1.1 kb, specific for *ipt* and spanned the *ipt* coding and termination regions from the T-DNA of octopine type plasmid 15955 (*29*). (**B**) Southern DNA hybridization from leaves of a tobacco plant obtained as progeny of a cross between transgenic clone 35*S-Ac-ipt* 12 and wild-type SR1. Samples, probe, and lanes as in (A). (**C**) Northern blot analysis of poly A$^+$ RNA extracted from transgenic leaves for the *ipt* RNA. Lane 1, RNA from clone 4 leaf tissues that were severely altered (*30*); lane 2, RNA from slightly altered leaf tissue (clone −5); lane 3, RNA from leaf tissue displaying strong alterations (clone −5); lane 4, RNA from leaf tissue severely altered (clone −19); lane 5, RNA from normal-looking leaf tissue from clone −19; and lane 6, RNA from severely altered leaf parts of plant clone 21. Two micrograms of poly(A)$^+$ RNA were loaded on each lane and separated on a 1.2% agarose-formaldehyde gel (*31*). (**D**) Northern blot analysis of total RNA (50 μg) extracted from adventitious buds of F_1 progeny of clone 5. The blot was hybridized to the *ipt*-specific probe. Lane 2 and 7, RNA extracted from teratoma-like buds; lanes 1, 3, and 8 RNA extracted from normal-looking or (lanes 4, 5, and 6) almost normal-looking buds.

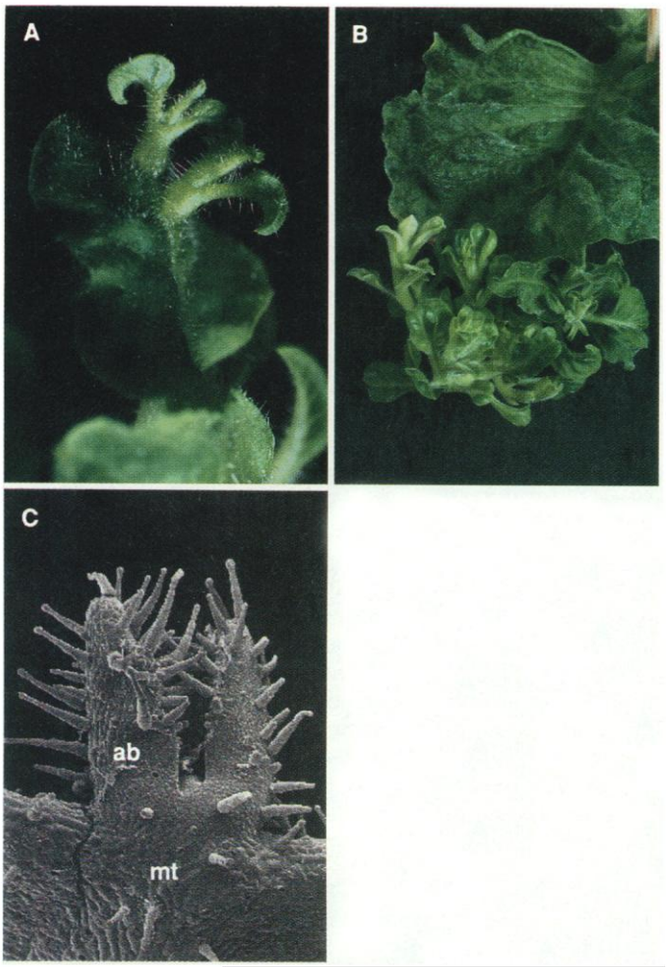

Fig. 3. Viviparous leaves in tobacco plants transgenic for the transposon-split 35*S-ipt* chimeric gene. (**A**) vegetative adventitious buds formed at the tip and in the middle of the leaf midrib in plant clone 35*S-Ac-ipt* 5. (**B**) Shoot grown out of an adventitious bud at the leaf tip of plant clone 35*S-Ac-ipt* 6. (**C**) Scanning electron micrograph of the leaf tip of a viviparous leaf transgenic for the 35*S-Ac-ipt* construct showing the emergence of an adventitious bud (ab) at the midrib tip (mt). The bud is 0.6 mm long.

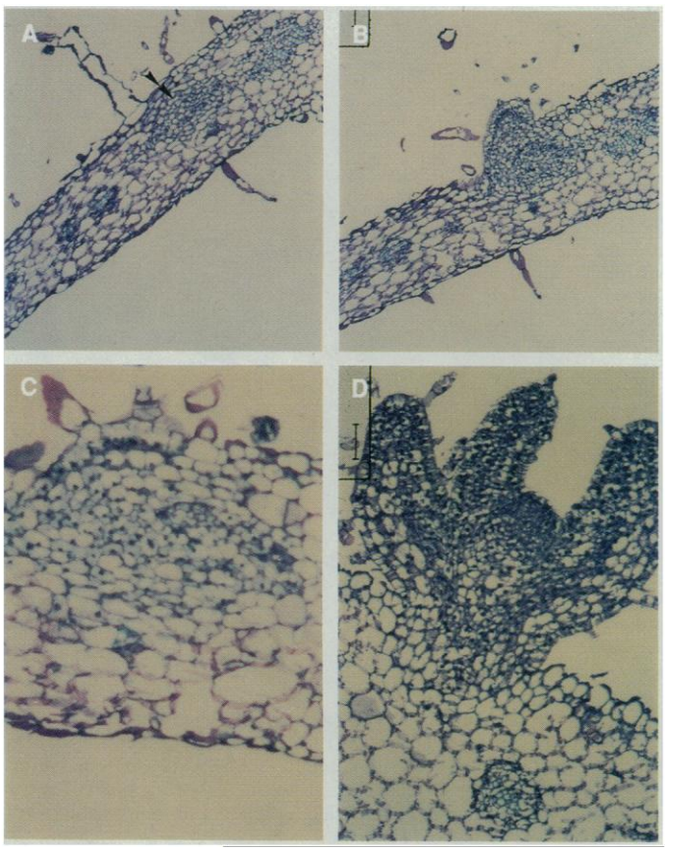

Fig. 4. Ontogenesis of adventitious buds in an F_1 progeny of 35*S-Ac-ipt* clone 5. Leaf sections showing direct organogenesis in a leaf. The bar line represents 0.1 mm. (**A**) Subepidermal cells in proximity of the vascular system divide to form a meristemoid tissue (arrow). (**B**) Later stage than (A), meristemoid tissue close to the leaf surface (×400). (**C**) Adventitious bud primordia. (**D**) Adventitious bud primordia emerging on the adaxial surface of the leaf.

a tissue is developmentally relevant.

We first observed vivipary of leaves during in vitro growth of two of the 20 35*S-Ac-ipt* transgenic shoots. Moreover, four out of the eight independent plant clones able to grow in soil (clones 35*S-Ac-ipt*-5, −6, −12, and −19) had viviparous leaves (Fig. 3, A and B). Viviparous leaves were also observed in 20 out of 60 kanamycin-resistant F1 progeny plants derived by crossing plants 35*S-Ac-ipt*-5 and −12 with SR1 wild-type plants. Under our experimental conditions, not all leaf cells exhibit the potential to generate a bud. Adventitious buds formed on the adaxial surface of the leaf vascular system, usually on midribs at the leaf tip (Fig. 3, A and C). Similarly, in vitro–induced organogenesis usually starts in cells located in the immediate proximity of veins (*17*). Histological analysis of viviparous leaves (Fig. 4) showed that adventitious buds arise from the subepidermal layer of the leaf cells (most likely parenchyma cells derived from LII), which agrees with results of other investigators (*18, 19*) that adventitious bud histogenesis cannot be traced exclusively to epidermal cells originated from the LI layer.

In plants, cell fate is believed to be determined by position and not by lineage (*20, 21*). Cells of the vascular parenchyma of tobacco leaves do not normally divide, and are committed to be a component of an organ with determinate growth. With transgenic tobacco plants, mosaic for the expression of a cytokinin-synthesizing gene, we have shown that cytokinin induces divisions in such cells, overriding the previous developmental plan and resulting in adventitious buds.

REFERENCES AND NOTES

1. M. T. Masters, *Vegetable Teratology* (Hardwick, London, 1869).
2. J. W. Goethe von, *Versuch. die Metamorphose der Pflanzen zu Erklären* (Gotha, Ettinger, 1790). The term "viviparous" best conveys the concept of fertility which is latent in the leaf, whereas the equivalent term "epiphylly" stresses more the heterotopic occurrence of structures such as shoots, leaves, and inflorescences on leaves.
3. T. A. Steeves and I. M. Sussex, *Patterns in Plant Development* (Cambridge Univ. Press, New York, 1989).
4. T. A. Dickinson, *Bot. Rev.* **44**, 181 (1978).
5. K. M. Tran Thanh Van, *Annu. Rev. Plant Physiol.* **32**, 291 (1983).
6. P. Zambryski, J. Tempe, J. Schell, *Cell* **56**, 193 (1989).
7. A. C. Smigocki and L. D. Owens, *Proc. Natl. Acad. Sci. U.S.A.* **85**, 5131 (1988).
8. J. J. Estruch and A. Spena, unpublished results.
9. J. I. Medford, R. Horgan, Z. El-Sawi, H. J. Klee, *Plant Cell* **1**, 403 (1989).
10. A. Spena, R. Hain, U. Ziervogel, H. Saedler, J. Schell, *EMBO J.* **4**, 2739 (1985).
11. T. Schmülling *et al.*, *FEBS Lett.* **249**, 401 (1989).
12. H. J. Klee, R. B. Horsch, M. A. Hinchee, M. B. Hein, N. L. Hoffmann, *Genes Dev.* **1**, 86 (1987).
13. A. Spena, *Trends Genet.* **6**, 76 (1990).
14. _____, R. D. Aalen, S. C. Schulze, *Plant Cell* **1**, 1157 (1989).
15. B. McClintock, *Carnegie Inst. Washington Publ.* **50**, 174 (1951) [in *The Discovery and Characterization of Transposable Elements*, J. A. Moore, Ed. (Garland,

New York, 1987), p. 214].
16. B. Baker, G. Coupland, N. Fedoroff, P. Starlinger, J. Schell, *EMBO J.* **6**, 1547 (1987).
17. E. M. Attfield and P. K. Evans, *J. Exp. Bot.* **42**, 51 (1991).
18. S. Satina, A. F. Blakeslee, A. G. Avery, *Am. J. Bot.* **27**, 895 (1940).
19. C. Broertjes and A. M. Van Harten, *Application of Mutation Breeding Methods in the Improvement of Vegetatively Propagated Crops* (Elsevier, Amsterdam, 1978).
20. H. Dermen, *Am. J. Bot.* **40**, 154 (1953).
21. R. N. Stewart and L. G. Burk, *ibid.* **57**, 1010 (1970).
22. E. W. Weiler, *Planta* **149**, 155 (1980).
23. J. Porath, F. Maisano, M. Belew, *FEBS Lett.* **185**, 306 (1985).
24. D. Rodbard, *Clin. Chem.* (*N.Y.*) **20**, 1255 (1974).
25. C. Koncz and J. Schell, *Mol. Gen. Genet.* **204**, 383 (1986).
26. J. Sambrook, E. F. Fritsch, T. Maniatis, *Molecular Cloning* (Cold Spring Harbor Laboratory, Cold Spring Harbor, NY, 1989).
27. The 4.7-kb Xba I bands are composed of the right part of the *Ac* transposable element plus the *ipt* coding and termination regions (see Fig. 1), and represent *Ac* donor sites. "Empty donor sites" (regions from which *Ac* has excised) are detected as bands of higher molecular weight in Xba I digests, and are reduced to bands of approximately 1.7 kb in Eco RI–Xba I double digests (large arrows). Bands indicated by small arrowheads are *Ac* donor sites, because they hybridize to *Ac*-specific probes, and they have a molecular weight higher than 4.7 kb most likely due to DNA methylation (*28*) of Xba I site (or sites) located at the 3′ end of the 35*S-Ac-ipt* construct.
28. M. A. Van Sluys, J. Tempe, N. Fedoroff, *EMBO J.* **6**, 3381 (1987).
29. R. F. Barker, K. B. Idler, D. V. Thompson, J. D. Kemp, *Plant Mol. Biol.* **2**, 335 (1983).
30. Leaves from 35*S-Ac-ipt* transgenic plants that present one or two small bulges are considered slightly altered, whereas those with either few big bulges or many small ones are said to be severely altered. The term "teratoma-like" refers to adventitious buds that develop abnormally giving tumorous masses.
31. The RNA blot was hybridized first to an *ipt*-specific probe (same as in panels A and B), and subsequently to an actin-specific probe to check that approximately equal amounts of polyA$^+$ RNA had been loaded on each lane. Molecular weight was calculated using a standard marker (BRL).
32. We thank S. Schwarz-Sommer for the scanning electron micrograph, P. Huijser for advice with the microscopical work, and S. C. Schulze for technical assistance. Supported by a European Molecular Biology Organization short-term fellowship to J.J.E. and the "Regeneration" European Economic Community project.

8 July 1991; accepted 2 October 1991

Structural Basis for the Activation of Glycogen Phosphorylase b by Adenosine Monophosphate

STEPHEN R. SPRANG,* STEPHEN G. WITHERS, ELIZABETH J. GOLDSMITH, ROBERT J. FLETTERICK, NEIL B. MADSEN

The three-dimensional structure of the activated state of glycogen phosphorylase (GP) as induced by adenosine monophosphate (AMP) has been determined from crystals of pyridoxalpyrophosphoryl-GP. The same quaternary changes relative to the inactive conformation as those induced by phosphorylation are induced by AMP, although the two regulatory signals function through different local structural mechanisms. Moreover, previous descriptions of the phosphorylase active state have been extended by demonstrating that, on activation, the amino- and carboxyl-terminal domains of GP rotate apart by 5°, thereby increasing access of substrates to the catalytic site. The structure also reveals previously unobserved interactions with the nucleotide that accounts for the specificity of the nucleotide binding site for AMP in preference to inosine monophosphate.

THE BURST OF CATABOLIC ACTIVITY that fuels rapid and continuous skeletal muscle contraction is sustained by glycogen phosphorylase (GP). Phosphorylase can be independently and coordinately activated by phosphorylation at Ser^{14} in response to hormonal and neuronal signals and by binding AMP (*1*). Phosphorylase occurs in vivo and in vitro as a stable dimer of 97.4-kD subunits related by a twofold axis of symmetry (*2*). On activation, dimers assemble into tetramers (*1*) in which the catalytic sites are occluded by dimer-dimer interactions (*3*). Glycogen is required to dissociate these tetramers into the fully active GP dimers found in vivo (*4*). The active state is also induced by sulfate ions (*5, 6*) which, at high concentration, mimic the phosphoserine group and bind to the AMP and catalytic sites (*7*).

Phosphorylation of GP (converting phosphorylase b, or GPb, into phosphorylase a, or GPa) is accompanied by a major conformational change in the amino terminus (*8*), which, as revealed by the structure of sulfate-activated GP, induces a rotation of subunits within the functional dimer (*3, 7*) that leads to the formation of activated tetramers. The mechanism by which AMP independently activates the dephosphorylated enzyme has not yet been described, since the only reported structure of the activated AMP complex (*3*) was determined from crystals grown in ammonium sulfate, which mimics the effects of phosphorylation. Consequently, it is not known whether AMP alone can induce the rearrangement of the amino terminus, with which it makes no direct contact, or promote the same quaternary structural changes induced by phosphorylation or sulfate ions. In order to resolve this question, we determined the structure of the pyridoxalpyrophosphoryl analog of phosphorylase b (PLPP-GPb) in a complex with AMP. The β-phosphate of the PLPP coenzyme analog occupies the substrate (orthophosphate) subsite in the catalytic site. In the absence of ligands, PLPP-GPb forms dimers. The equilibrium conformation of this molecule, as measured by its affinity for adenosine 5′-monothiophosphate (dissociation constant K_d = 40 μM), is similar to that of the native dephosphorylated enzyme in the presence of saturating glucose-1-phosphate (K_d = 140 μM). Its conversion to the active tetrameric state requires AMP (*9, 10*).

The structure of the tetrameric complex with AMP has been determined by x-ray crystallography to a resolution of 3.0 Å. Orthorhombic crystals (*11*) of PLPP-GPb were grown by using polyethylene glycol 8000 as a precipitant. These crystals can only be obtained in the presence of AMP and differ from the monoclinic form of GP grown in 1.0 M ammonium sulfate (*7*). A complete set of x-ray diffraction data to 3.0 Å was measured and processed as described (*11*) (Table 1). The structure was determined by molecular replacement, and the atomic model was refined to a crystallographic *R* factor of 0.18 with data between 8.0 and 3.0 Å resolution (*11*) (Table 1).

The four subunits of the PLPP-GPb tetramer are related by noncrystallographic molecular 222 symmetry as reported for activated GPb (*3*). Tetramers are formed by isologous interaction between dimers. The average root-mean-square (rms) deviation between subunits, after superposition of all equivalent Cα atoms, is ~0.6 Å (Table 2). Superpositions in which only the β-sheet core residues (*12*) of the subunits were used yielded an rms deviation of less than 0.32 Å, slightly greater than the estimation of coordinate error (0.3 Å) by the method of Luzatti (*13*). Comparisons among previously determined phosphorylase structures (Ta-

S. R. Sprang, Howard Hughes Medical Institute and Department of Biochemistry, University of Texas Southwestern Medical Center, Dallas, TX 75235–9050.
S. G. Withers, Department of Chemistry, University of British Columbia, Vancouver, BC V6T 1Y6.
E. J. Goldsmith, Department of Biochemistry, University of Texas Southwestern Medical Center, Dallas, TX 75235–9050.
R. J. Fletterick, Department of Biochemistry and Biophysics, University of California, San Francisco, CA 94143.
N. B. Madsen, Department of Biochemistry, University of Alberta, Edmonton, Alberta T6G 2H7.

*To whom correspondence should be addressed.